ceramics

MDPI

Article

Mussel-Inspired Construction of Silica-Decorated Ceramic Membranes for Oil–Water Separation

Qibo Zhou [1,2], Qibing Chang [3], Yao Lu [1] and Jing Sun [2,*]

[1] School of Materials Science and Engineering, Shenyang University of Chemical Technology, Shenyang 110142, China; 13238933338@163.com (Q.Z.); luyao915@syuct.edu.cn (Y.L.)
[2] State Key Laboratory of High Performance Ceramics and Superfine Microstructure, Shanghai Institute of Ceramics, Chinese Academy of Sciences, 1295 Dingxi Road, Shanghai 200050, China
[3] School of Materials Science and Engineering, Jingdezhen Ceramic University, Jingdezhen 333403, China; changqibing@jcu.edu.cn
* Correspondence: jingsun@mail.sic.ac.cn

Abstract: In recent years, ceramic membranes have received widespread focus in the area of liquid separation because of their high permeability, strong hydrophilicity, and good chemical stability. However, in practical applications, the surface of ceramic membranes is prone to be contaminated, which degrades the permeation flux of ceramic membranes during the separation process. Inspired by mussels, we imitate the biomimetic mineralization process to prepare a ceramic membrane of nano–silica on the pre-modified zirconia surface by co-deposited polydopamine/polyethyleneimine. The modified ceramic membranes were utilized for the purpose of oil–water separation. Separation performance has been tested using a disc ceramic membrane dynamic filtration device. The outcomes revealed an enhanced permeability in the modified membrane, measuring as 159 L m^{-2} h^{-1} bar^{-1}, surpassing the separation flux of the unmodified membrane, which was 104 L m^{-2} h^{-1} bar^{-1}. The permeation performance of the modified membrane was increased to 1.5 times. Modified ceramic membranes are highly resistant to fouling. From the beginning to the end of separation process, the oil rejection rate of the modified ceramic membrane is always higher than 99%. After a 2 h oil–water separation test run, modified ceramic membrane permeate flux can be restored to 91% after cleaning. It has an enormous capacity for application in the area of oil–water separation.

Keywords: ceramic membrane; polydopamine; silicification; oil–water separation

Citation: Zhou, Q.; Chang, Q.; Lu, Y.; Sun, J. Mussel-Inspired Construction of Silica-Decorated Ceramic Membranes for Oil–Water Separation. *Ceramics* **2024**, *7*, 250–263. https://doi.org/10.3390/ceramics7010016

Academic Editor: Gilbert Fantozzi

Received: 29 November 2023
Revised: 26 January 2024
Accepted: 19 February 2024
Published: 22 February 2024

1. Introduction

Global water scarcity has been a persistent issue for an extended period, which refers to the phenomenon when regional or global societies are unable to meet their water needs [1]. It is a huge challenge that affects human health, agriculture, industry, ecosystems, and sustainable development [2]. The causes of water scarcity are complex and varied, including population growth, climate change, over-abstraction of groundwater, water pollution, and ecosystem destruction. Among them, pollution caused by oily wastewater has a very significant impact on water resources [3]. The effects of this pollution not only ripple through aquatic ecosystems, but also pose a huge challenge to the safety of drinking water.

During industrial production and processing, a large amount of oily wastewater is generated. These oily wastewater typically come from industrial fields such as oil production, petroleum refining, chemical engineering, metal processing, and food processing. It contains a large amount of oils, petroleum substances, or organic compounds [4]. Oily wastewater is highly polluted and difficult to treat, resulting in serious environmental impacts that require special treatment to meet emission standards or the requirements of recycling [5]. In general, the size of oil droplets in oily wastewater is extremely minute, especially in oil-in-water emulsions, which can reach the nano scale [6]. The effect of conventional oil–water separation can hardly meet the emission standards of oil-in-water

emulsion [7,8]. Membrane separation technology has emerged as a key technology to solve this problem [9,10]. The working principle of membrane separation refers to the selective separation of mixtures of different particle sizes at the molecular level when passing through a membrane. According to the pore size, membranes can be divided into microfiltration membrane (MF), ultrafiltration membrane (UF), nanofiltration membrane (NF), and reverse osmosis membrane (RO), etc. Membrane separation includes staggered dynamic filtration or dead-end filtration [11]. Scholars are more focused on membrane separation technology in comparison to traditional oil–water separation methods, owing to its notable advantages such as excellent separation efficiency, minimal power consumption, and ease of handling [12]. Ceramic membrane, as a typical inorganic membrane material, has advantages such as high chemical stability and excellent damage resistance. Ceramic membranes can operate in a variety of extreme environments, which is not possible with organic membranes [13,14]. The ceramic membrane itself has excellent hydrophilicity, making it highly permeable.

However, throughout the process of oil–water separation, ceramic membranes frequently confront contamination issues posed by oil droplets [15,16]. To solve this problem, scholars are committed to the study of membrane surface modification to improve its permeation performance and contamination resistance. SiO_2 [17], TiO_2 [18] and other minerals with hydrophilicity and underwater oleophobicity have become ideal candidates as coating materials. Chang et al. [19] coated an industrial ceramic membrane with nano-TiO_2 to enhance its hydrophilicity. This modification proved effective when the oil concentration in the feed material did not exceed 4 g/L, the concentration of oil in the filtrate did not surpass 10 mg/L. Meng et al. [20] achieved hydrophilic and lipophilic properties by depositing silica nanoparticles onto the porous membranes and grafting chlorotrimethylsilane and perfluorinated surfactants on the modified surface of silica nanoparticles, respectively. These modifications resulted in membranes with good separation performance.

Membrane surface modification can be done by hydrothermal [21], sol-gel [22,23], and impregnation [24,25] methods. However, since the ceramic membrane surface contains only a small amount of hydroxyl groups, the bond between the functional layer and the ceramic membrane is not strong enough. In the process of separating oil and water, the functional layer of ceramic membranes is prone to be contaminated, posing challenges in achieving consistent and stable performance. Inspired by the formation of mussels, dopamine can adhere to organic or inorganic surfaces with a simple deposition process [26]. Under conditions of mild alkalinity, dopamine can undergo oxidative self-polymerization to form polydopamine, which contains a large number of hydroxyl and amino groups on its surface. A large number of reactive groups can make the ceramic membrane surface easier to be modified. Liu et al. [27] prepared polyimide nanofiber membranes using polydopamine and polytetrafluoroethylene. Fiber membranes were modified to possess extreme water repellency and high oil affinity, resulting in a flux of up to 6000 L m^{-2} h^{-1} bar^{-1}. Also, the oil resistance rate can reach more than 99% and can be operated stably under extreme environments. Gao et al. [28] prepared a new membrane with switchable super-wettability using dopamine coating and chemical grafting. The prepared membrane could realize hydrophobic-hydrophilic conversion by soaking in hydrochloric acid solution (pH = 1) and ethanol. The membrane exhibits a permeate flux capability of 186.12 L/m^2 h at pH = 1. The modified membrane is well-suited for the efficient separation in environments with strong acidity. Li et al. [29] prepared a multifunctional fiber membrane with dual wettability by attaching zinc oxide to the membrane surface using polydopamine. The modified membranes can provide rapid separation of emulsions, and the separation efficiency is always higher than 99%.

There are also problems if only polydopamine is used for deposition. The duration for depositing polydopamine onto the ceramic membrane is excessively prolonged, prone to the formation of agglomerated particles resulting in reducing the size of the pores in the ceramic membrane, affecting the efficiency during the process of separation. To tackle the issues raised earlier, many studies had co-deposited dopamine and polyethyleneimine

on the surface of membranes, which established as a viable strategy to enhancing the efficiency of ceramic membrane performance [30]. Due to its abundant amino groups, polyethyleneimine has the capability to undergo Schiff base and Michael addition reactions with polydopamine. This improves its hydrophilicity and prevents aggregation [31]. Yang et al. [32] used polydopamine and polyethyleneimine co-deposited atop the surface of microfiltration membranes made of polypropylene, and the deposition time of the co-deposited membranes was greatly reduced and the hydrophilicity was enhanced, as compared to membranes deposited only with polydopamine. The separation of oil-in-water emulsions can be performed under atmospheric pressure conditions and oil drainage rate as high as 98%. Luan et al. [33] introduced tertiary amines on the membrane through a co-deposited layer of polydopamine/polyethyleneimine, which were utilized for the quaternization reaction with 2-bromoethanesulfonate. The amphiphilic-modified ceramic membranes showed good hydrophilicity. The water contact angle may achieve a maximum value of 20.5°. The modified ceramic membrane provided twice the permeation flux (40 L m^{-2} h^{-1} bar^{-1}) of the unmodified membrane (20 L m^{-2} h^{-1} bar^{-1}) when separating oil-in-water emulsion. Zhao et al. [34] prepared a co-deposited coating of dopamine and polyethyleneimine on the surface of Al_2O_3 membrane, and crosslinked with glutaraldehyde to prepare a composite ceramic nanofiltration membrane for high-temperature desalination application. The retention performance of the modified ceramic membrane for divalent cations was more than 91%. At the same time, the permeate flux under 0.5 MPa reached 21 L m^{-2} h^{-1}. Modified membranes exhibit good desalination performance. Song et al. [35] utilized a non-solvent induced phase separation technique to prepare polyvinylidene fluoride/polydopamine/polyethyleneimine composite membranes on polyester nonwoven fabrics. The membrane was peeled off from the support, and the upper layer of the membrane was hydrophilic and the lower layer of the membrane was hydrophobic. The contact angle of underwater oil in the upper layer of the modified membrane was 152.2°, while the contact angle of under oil water in the lower layer of the modified membrane was 153.3°. The modified membrane could be used for unidirectional oil–water separation. This study proposed a strategy of preparing a nano silica layer prepared on a ceramic membrane surface modified by co-deposited polydopamine/polyethyleneimine (PDA/PEI). Using the ZrO_2 disc ceramic membrane as a substrate, the bonding process involving the Schiff base reaction and Michael addition reaction between PDA and PEI was utilized to co-deposit on the disc ceramic membrane surface. Through biomimetic mineralization [36], tetramethyl orthosilicate (TMOS) is hydrolyzed to orthosilicic acid, which formed a layer of nano-silica on a disc ceramic membrane. The excellent hydrophilicity and underwater oleophobicity of nano silica are utilized to enhance the separation efficiency and contamination resistance of the membrane during operation. The microstructure of original and modified membrane was characterized using FTIR, XPS, and AFM. Tests were additionally carried out on the ceramic membranes subjected to modifications to separate oil-in-water emulsions, and their permeation flux, efficiency of separation, and anti-fouling ability were analyzed. An effective method is provided for designing and manufacturing ceramic membranes with anti-fouling properties.

2. Experiment

2.1. Materials

ZrO_2 disc ceramic membranes (CM, compact disc shape, internal diameter 40 mm, external diameter 200 mm, thickness 6 mm) were derived from Chongqing Vauxton Nano Tech Co., Ltd. (Chongqing, China), the shape of the membrane is shown in Figure 1. Dopamine (DA) hydrochloride, polyethyleneimine (PEI 600 Da), tetramethyl orthosilicate (TMOS), tris(hydroxymethyl)- aminomethane, n-hexane, and petroleum ether were purchased from Shanghai Adamas Reagent Co., Ltd. (Shanghai, China). Sodium dihydrogen phosphate, dibasic sodium phosphate and hydrochloric acid (GR, 36–38%) were purchased from Shanghai Titan Scientific Co., Ltd. (Shanghai, China). Kerosene was acquired from Tianjin Yuanli Chemical Reagent Co., Ltd. (Tianjin, China). Diesel oil was procured from

Sinopec Shanghai Petrochemical Co., Ltd. (Shanghai, China). The soybean oil was purchased from Arowana. Tween-80 and Span-80 were acquired from Sinopharm Chemical Reagent Co., Ltd. (Shanghai, China). Anhydrous ethanol was acquired from Shanghai Lingfeng Chemical Reagent Co., Ltd. (Shanghai, China). All experiments were conducted using deionized water produced in the laboratory.

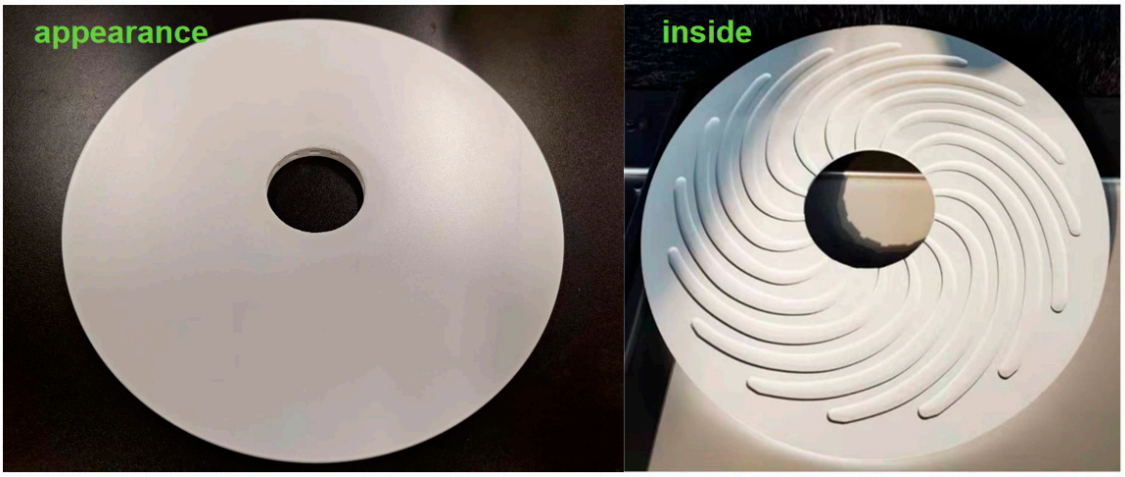

Figure 1. Pictures of ZrO_2 disc ceramic membrane.

2.2. Preparation of Modified Ceramic Membranes

The modified ceramic membrane was prepared as follows [37]. The Schiff base reaction and Michael addition reaction were utilized to enable the creation of a co-deposited layer consisting of polydopamine (PDA) and polyethyleneimine (PEI) on the ceramic membrane surface. ZrO_2 disc ceramic membranes underwent pre-wetting in deionized water for 6 h, followed by drying at 40 °C for 12 h in a vacuum oven. Dopamine hydrochloride (2 g/L) and polyethyleneimine (2 g/L) were added into the prepared Tris-HCl buffer solution (pH 8.5, 50 mM) and thoroughly stirred for uniform distribution. The pre-selected prepared ZrO_2 membranes were submerged in the mixed solution and reacted at 25 °C for different period of time. The modified membranes were rinsed with deionized water and subsequently dried in an oven at 40 °C for 8 h. The ceramic membrane after the PDA/PEI co-deposition reaction was named as CM-PDA/PEI.

Tetramethyl orthosilicate and HCl solution (1 mM) were combined in a volume ratio of 1:50 and mixed for 30 min. Then, it was combined with an equal volume of phosphate-buffered solution (0.2 M, pH = 6.0). CM-PDA/PEI was placed into the modified solution and reacted at 25 °C for different period of time. After the reaction, the ceramic membranes underwent rinsing with deionized water, and were subsequently dried in a vacuum oven at 40 °C for 12 h. The final ceramic membrane obtained was referred to as CM-PDA/PEI-SiO_2. The modification process of the membrane was prepared, as shown in Figure 2.

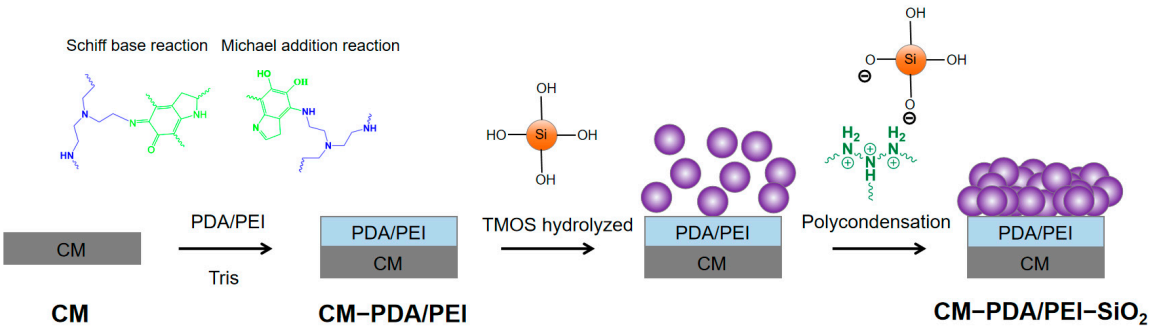

Figure 2. Illustrative diagram of modified ceramic membrane preparation.

2.3. Characterization of the Membrane

The surface morphology of the ceramic membranes at various stages was observed by field emission scanning electron microscope (FESEM, SU8220, HITACHI, Tokyo, Japan). Changes in surface roughness were characterized using an atomic force microscope (AFM, NT–MDT, Moscow, Russia). The distribution of pore sizes in the ceramic membranes, both before and after modification, was determined using an ultrafiltration membrane pore size analyzer (PSMA-10, Nanjing Gaoqian Functional Materials Tech Co., Ltd., Nanjing, China). The element compositions on the surface of both the original ceramic membranes, and the modified ceramic membranes were analyzed by an X-ray photoelectron spectrometer (XPS, ESCAlab250, Thermo Fisher Scientific, Waltham, MA, USA). The alterations in functional groups on the ceramic membranes surface were analyzed using a Fourier transform infrared spectroscope (FTIR, IS–20, Nicolet, Madison, WI, USA). The water contact angle (WCA) and underwater oil contact angle (UOCA) on the surface of ceramic membranes were measured by a contact angle measuring instrument (CA, OCA 20, Dataphysics, Filderstadt, Germany).

2.4. Membrane Separation Performance

The reaction density was utilized to determine the time required for the reaction [38]. The reaction density was calculated by Equation (1):

$$RD = \frac{G_R - G_0}{S} \quad (1)$$

where RD stands for reaction density, G_0 is the weight (mg) of the original ceramic membrane, G_R is the weight (mg) of the membrane at the end of the reaction, and S is the reaction area (cm^2).

The separation efficiency of both the unmodified and modified disc ceramic membranes was characterized using a disc ceramic membrane dynamic filtration device (TD-WD-001, Anhui Transcendent New Materials Technology Co., Ltd., Anhui, China). In the operation process, the permeate is pumped into the disc ceramic membrane dynamic filtration device, which is regulated with a speed motor. The permeate speed is regulated by the rotational speed of disc ceramic membrane, and the permeate is separated through the membrane. The permeation performance of ceramic membranes was tested. The membrane permeability was determined using Equation (2):

$$Q = \frac{V}{A \times t \times P} \quad (2)$$

where Q stands for permeability, V is the volume (L) of permeated water through the membrane, A is the actual area (m^2) used in the separation process, t is the running time (h), and P is the transmembrane pressure (bar).

The oil phase utilized soybean oil in this experiment, the aqueous phase consists of deionized water. Tween-80 and Span80 are emulsifiers. The concentration of the oil is measured using an ultraviolet spectrophotometer (UV-1610, Beijing Ruili Instrument Co., Ltd., Beijing, China) [39]. The oil rejection rate of oil (R) was calculated using Equation (3):

$$R = \left(\frac{C_0 - C_p}{C_0}\right) \times 100\% \quad (3)$$

where C_0 represents the initial oil concentration of the original oil-in-water emulsion and C_p represents the oil concentration after being filtrated.

3. Results and Discussion

3.1. Microstructure and Chemical Composition of Ceramic Membrane Surface

A series of characterizations were performed to investigate whether CM-PDA/PEI-SiO_2 was successfully generated. Figure 3 shows the optimal reaction time for the modified ceramic membrane. The reaction density of the PDA/PEI co-deposition reaction

increased rapidly in the first 4 h. After 4 h, the reaction density did not change much. The co-deposition reaction is therefore considered to be saturated after 4 h. Similarly, the modification of the nano silica layer showed almost no change after 8 h. For all samples subsequently tested, the PDA/PEI co-deposition time was 4 h and nano silica coating modification time was 8 h.

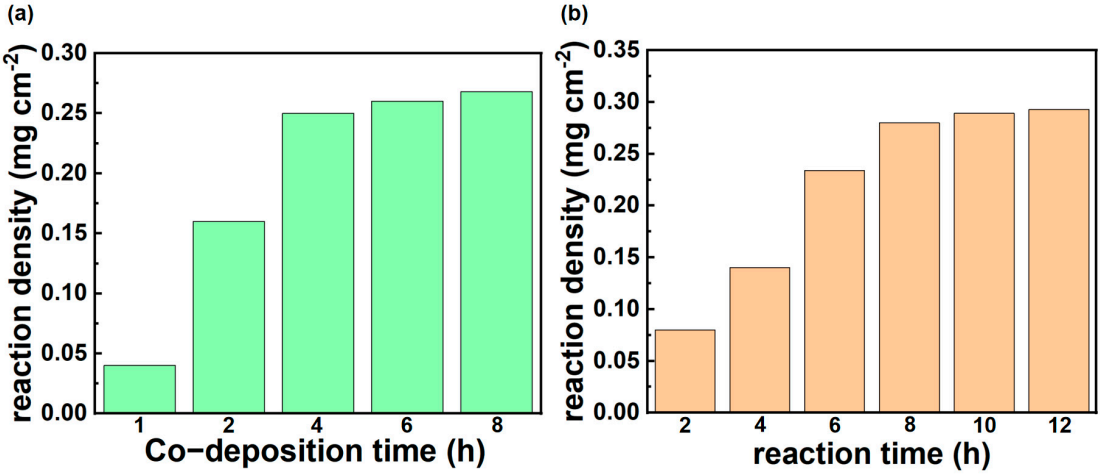

Figure 3. (**a**) Reaction density of the PDA/PEI co–deposition reaction at different time; (**b**) reaction density for the formation of nano silica at different time.

FTIR characterized the changes on functional groups of membrane. The findings were presented in Figure 4. Compared to CM, CM–PDA/PEI showed the telescopic vibrational peak of C=O in PDA at 1730 cm^{-1}. The introduction of PDA and PEI resulted in the appearance of N–H bonds at 3626 cm^{-1}. Due to the Schiff base reaction and Michael addition reaction between PDA and PEI, the C=N peak appeared at 1655 cm^{-1}. After the modification was completed, the peak of Si–O–Si appeared at 1077 cm^{-1}. This is due to the hydrolysis of TMOS into protosilicic acid, which forms a silica nanolayer grown on the surface of the ceramic film in phosphate buffer. The results showed that nano silica modified PDA/PEI co-deposited ceramic membranes were successfully prepared.

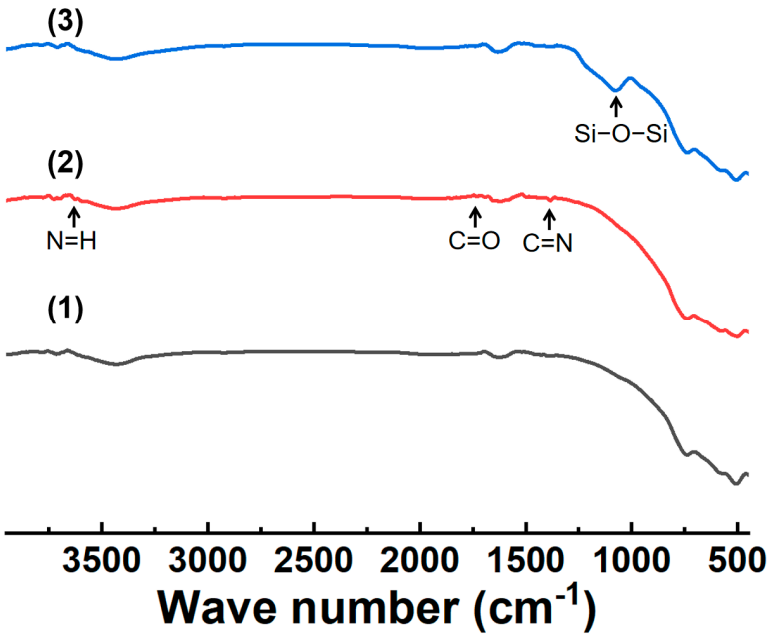

Figure 4. FTIR spectra of different membranes: (1) CM; (2) CM–PDA/PEI; (3) CM–PDA/PEI–SiO_2.

XPS analysis was employed for further characterization of the surface composition. The results are shown in Figure 5; compared to the CM, the peak of N1s appeared on the surface of CM–PDA/PEI [40], while the peak of Zr3d became weaker, which was caused by the fact that PDA and PEI contained N elements and PDA/PEI formed a co–deposited layer covering the original ceramic membranes surface. The peak of Si2p3 appeared on the CM–PDA/PEI–SiO_2 surface, which proved that nano silica was successfully modified on the surface.

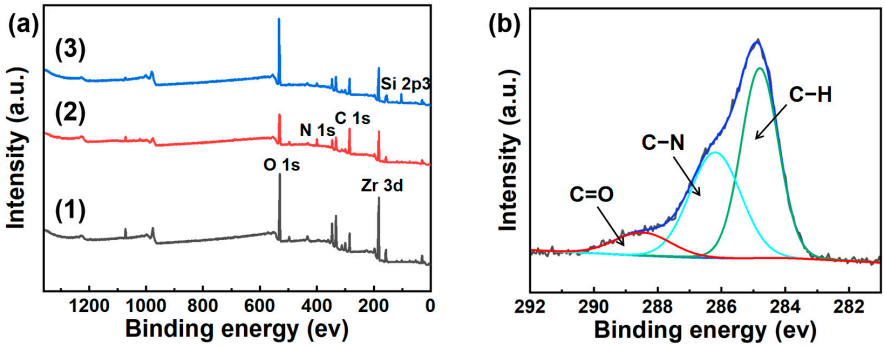

Figure 5. (**a**) XPS spectra of different membranes: (1) CM; (2) CM–PDA/PEI; (3) CM–PDA/PEI–SiO_2; (**b**) C1s spectra of CM–PDA/PEI–SiO_2.

The surface morphology of the prepared membranes characterized with FESEM was shown in Figure 6. After modification, PDA and PEI were uniformly deposited on the CM. The membrane pore size decreased slightly after modification. Also, no aggregated particles of polydopamine were found in the modified ceramic membrane. The change brought by the modification were in nano-scale, and there was no phenomenon of blocking the pores, which hardly reduced the permeation flux of the ceramic membrane. Figure 7 shows the elemental distribution of the modified ceramic membrane analyzed using EDS spectroscopy. Zr, N, and Si elements were evenly distributed on the surface of the CM–PDA/PEI–SiO_2. AFM was utilized to observe changes in roughness (Figure 8). The roughness of the CM was 121.1 nm. After the formation of a co–deposited layer on the ceramic membrane surface with PDA/PEI, the roughness increased to 141.5 nm. Upon the formation of a nano-silica layer, the roughness reached 151.9 nm. The augmented roughness facilitates the retention of a substantial amount of water on the ceramic membrane surface, resulting in the creation of a hydration layer. This, in turn, enhances permeability and anti-fouling capabilities of the ceramic membrane, ultimately achieving the intended separation effectiveness [41]. The average pore size of the CM was 104 nm, while the CM–PDA/PEI–SiO_2 exhibited an average pore size of 90 nm (Figure 9), respectively. It is noteworthy that the nanoscale modification had minimal impact on the pore size of the membranes. This change hardly affects the permeability of the ceramic membrane during use. This is consistent with the test results in Figure 6.

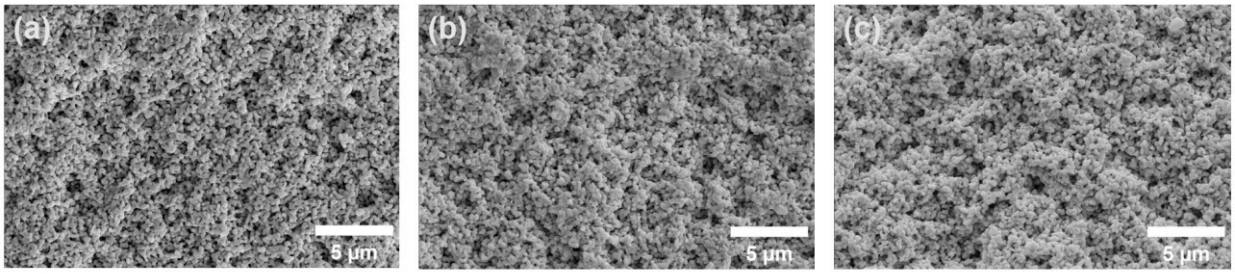

Figure 6. FESEM images of (**a**) CM; (**b**) CM–PDA/PEI; (**c**) CM–PDA/PEI–SiO_2.

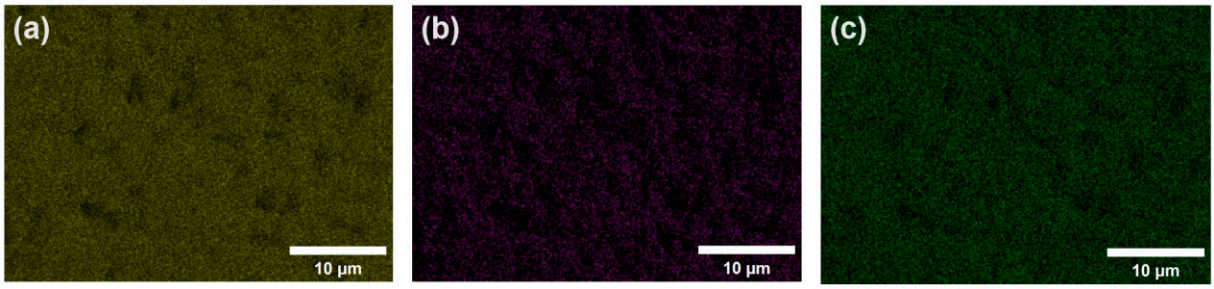

Figure 7. Elemental distribution of modified membrane after coating by nano SiO_2 (**a**) Zr; (**b**) N; and (**c**) Si.

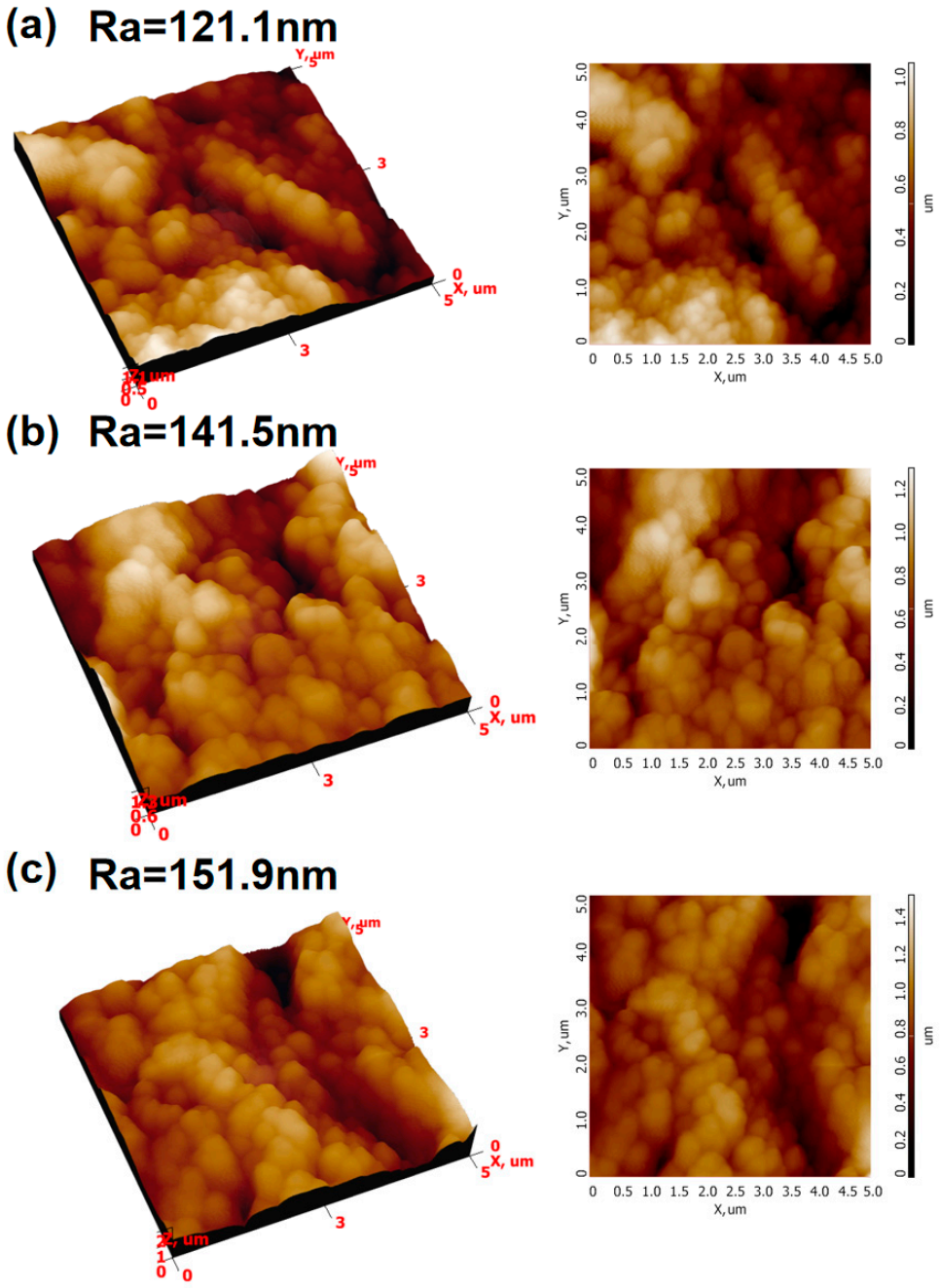

Figure 8. AFM images of (**a**) CM; (**b**) CM–PDA/PEI; and (**c**) CM–PDA/PEI–SiO_2.

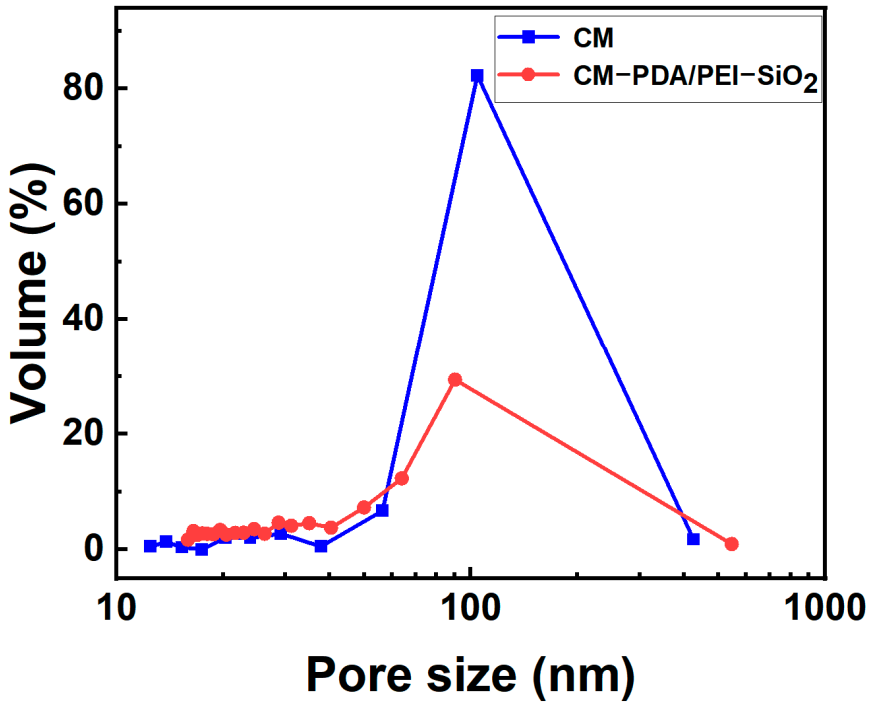

Figure 9. Distributions of pore sizes for CM and CM–PDA/PEI–SiO_2.

3.2. Contamination Resistance of Ceramic Membrane Surfaces

The hydrophilicity of the ceramic membrane was assessed through the measurement of its contact angle. The result was shown in Figure 10a–f, the WCA of the CM was 37.6°, the WCA of the CM–PDA/PEI was 41.1°, while the CM–PDA/PEI–SiO_2 exhibited a WCA of 28.5°, and the modified ceramic membrane showed good wettability. The UOCA of the CM, CM–PDA/PEI, and CM–PDA/PEI–SiO_2 was measured using soybean oil to determine the oleophobic properties. The UOCA of the CM, CM−PDA/PEI, and CM–PDA/PEI–SiO_2 were measured at 155.8°, 157.4°, and 159.1°, respectively. The modified ceramic membrane has better oleophobic properties. Due to the modification, it can show better anti-fouling ability in practical application scenarios. Meanwhile, the UOCA of the CM–PDA/PEI–SiO_2 was measured with several different oils, as shown in Figure 10g. The UOCA of the modified ceramic membranes measured with n–hexane, kerosene, diesel oil, and petroleum ether as oil phases were 157.4°, 154.8°, 159.2°, and 159.4°, respectively. Modified ceramic membranes keep the similar hydrophobic properties for oily wastewater and can be used in a wide variety of operating environments.

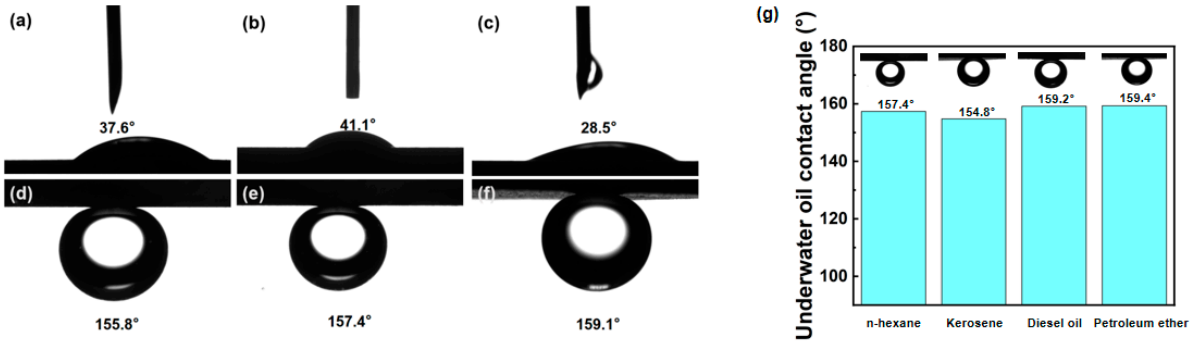

Figure 10. The WCA of (**a**) CM; (**b**) CM–PDA/PEI; (**c**) CM–PDA/PEI–SiO_2. The UOCA of (**d**) CM; (**e**) CM–PDA/PEI; (**f**) CM–PDA/PEI–SiO_2; (**g**) the UOCA of CM–PDA/PEI–SiO_2 for different types of oils.

Figure 11 shows the full view of the dynamic filtration device and the measurement of pure water permeability of ceramic membranes using a dynamic filtration device. The rotational period of the device was 365 r/min. The actual area used in the separation process is 0.0625 m^2. The trans-membrane pressure was 1 bar. Measurements were started after the device had been in stable operation for 30 min. The results are shown in Figure 12. The permeability of the CM was 532 L m^{-2} h^{-1} bar^{-1}, and after modification, the permeability decreased to 510 L m^{-2} h^{-1} bar^{-1}. It was due to the smaller average pore size after modification, as shown in Figure 9, which led to a slight decrease in the permeability. This is consistent with the conclusions drawn earlier in Figure 6. There is no dramatic difference on the separation performance of ceramic membranes.

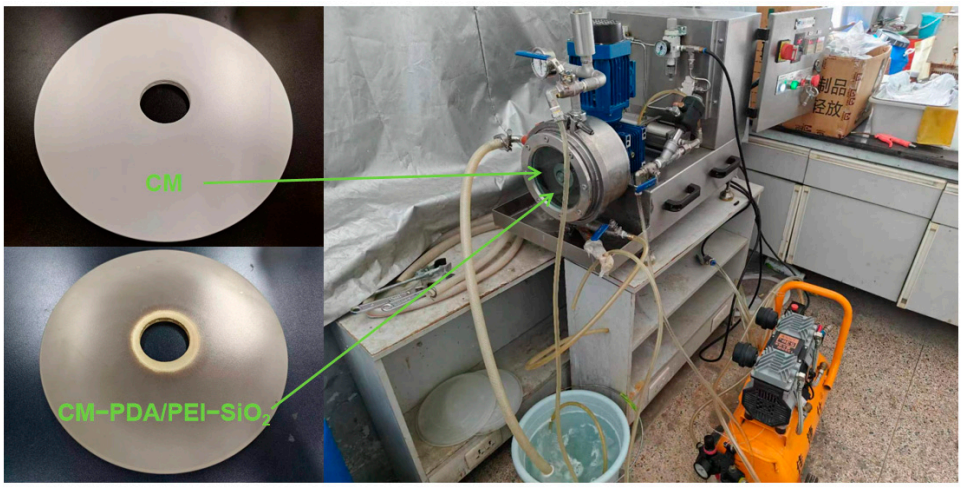

Figure 11. The full view of the dynamic filtration device.

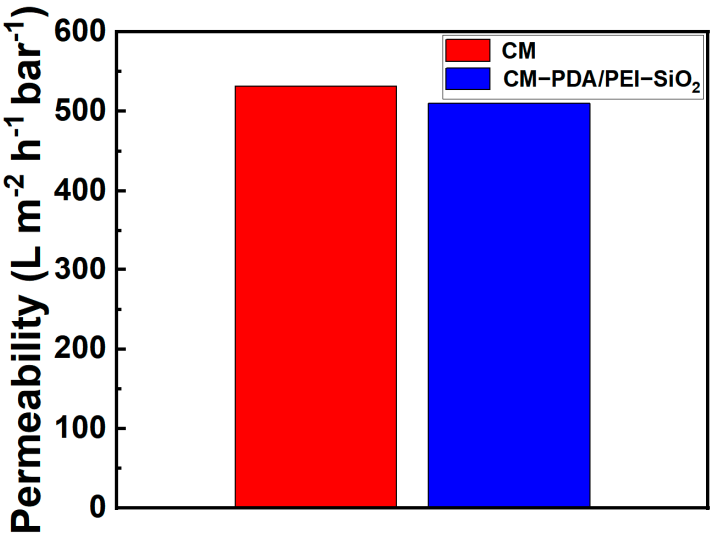

Figure 12. The permeability of ceramic membranes for pure water.

The separation performance of ceramic membranes on oil–in–water emulsion was measured to test the resistance of ceramic membranes to contamination in practical applications. The oil concentration of the oil–in–water emulsion was 0.5 g/L. The device was operated for 2 h. As shown in Figure 13, due to membrane contamination, the permeate flux of the CM exhibited a notable decrease within the initial 20 min, and the permeability of the CM decreased from the initial 145 L m^{-2} h^{-1} bar^{-1} to 104 L m^{-2} h^{-1} bar^{-1}. The permeability of the CM–PDA/PEI–SiO_2 decreased from the initial 226 L m^{-2} h^{-1} bar^{-1} to 159 L m^{-2} h^{-1} bar^{-1}. After running for some time, the permeability gradually tends

to stabilize; this is due to the fact that soybean oil forms a droplet layer on the membrane at the beginning of oil–water separation. The droplet layer can reduce new membrane contamination [42], slowing down the rate of membrane contamination. The permeate flux of the CM–PDA/PEI–SiO_2 was always higher than that of the CM during the operation. This is due to the nano-silica layer having strong oil resistance properties, and prevents the formation of a continuous oil layer, making the modified ceramic membrane more resistant to contamination than the unmodified ceramic membrane. In comparison to CM, the oil rejection rate of CM–PDA/PEI–SiO_2 at the beginning of the operation was always above 99%, and can be operated stably for 2 h. In contrast, the oil rejection rate of the original ceramic membranes is only 90.5%, and the ideal separation efficiency could only be achieved after a period of operation. The imaging of the original oil–in–water emulsion and the permeate after filtration with CM–PDA/PEI–SiO_2 under an optical microscope is shown in Figure 14a. The particle size distribution of the oil-in-water emulsion is shown in Figure 14b. The mean particle size of the oil-in-water emulsion was 182.4 nm. The feed solution exhibited a significant presence of oil droplets. After filtration, oil droplets were almost invisible. The excellent separation efficiency of the modified ceramic membrane was evident. Following the filtration of the oil-in-water emulsion, the ceramic membranes underwent a cleaning process, and the permeability with pure water was subsequently measured. Measure the pure water fluxes of CM and CM–PDA/PEI–SiO_2 again. The pure water permeability of CM and CM–PDA/PEI–SiO_2 were restored to 72% and 91%, respectively, of the pure water fluxes before the filtration experiments. CM–PDA/PEI–SiO_2 has a longer working life compared to CM. The variance in filtration performance among the membranes stemmed from differences in their surface properties. The modified ceramic membrane has great permeate flux and anti-fouling capabilities, and due to the modification of silica, can effectively inhibit the contamination of oil for the ceramic membrane. This prolongs the service life of the ceramic membrane.

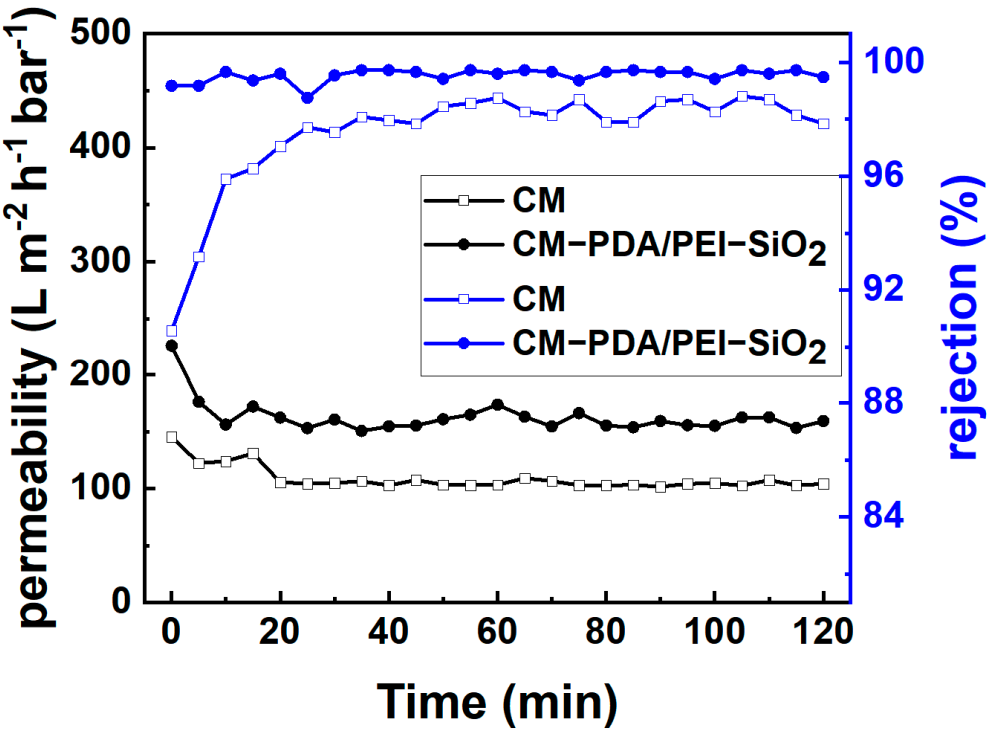

Figure 13. Variation of ceramic membrane permeability and rejection in the filtration process.

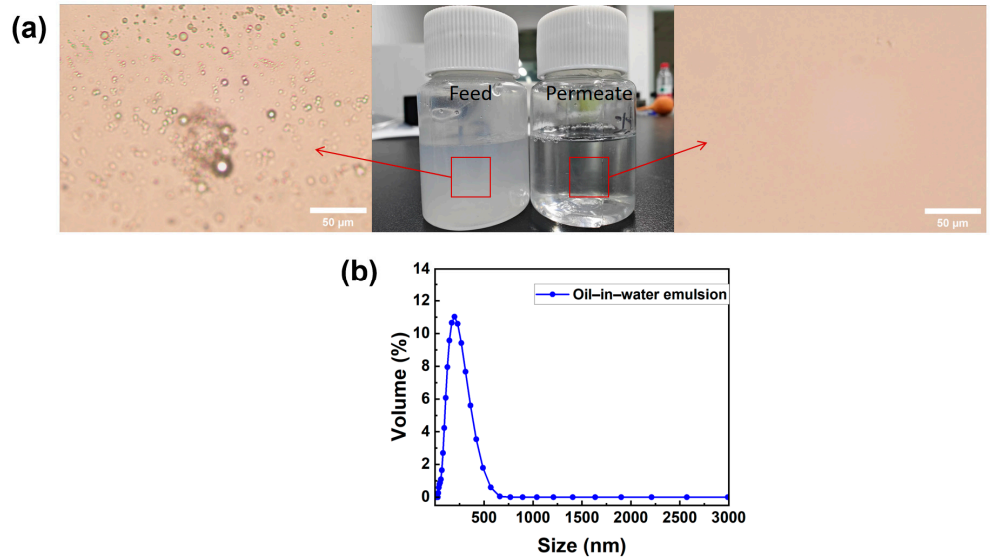

Figure 14. (**a**) Imaging of oil–in–water emulsions under optical microscope before and after modified ceramic membrane filtration. (**b**) Particle size distribution of oil–in–water emulsions.

4. Conclusions

In this study, nano silica modification was successfully carried out on the surface of CM using co–deposition of PDA/PEI. PDA/PEI was used as an intermediate layer for the bonding components, and silica-decorated coatings were introduced as a further functionalized layer. The silica-modified PDA/PEI co–deposited ceramic membrane was thus obtained. The modified ceramic membranes show better separation efficiency and contamination resistance than the original ceramic membranes. The silica-decorated ceramic membrane permeability is 1.5 times higher than the original ceramic membrane flux, while its oil rejection rate is always higher than 99%. CM–PDA/PEI–SiO_2 also had better cycling performance than CM. This was due to the fact that the inherent underwater oil resistance of silica inhibits oil droplets from causing membrane contamination on the ceramic membrane surface, thus preventing oil contamination. In summary, this study provides an effective method to prepare anti-fouling ceramic membranes for oil–water separation, which is conducive to prolonging the service life and decreasing the operating cost in practical applications.

Author Contributions: Q.Z.: Conceptualization, Methodology, Investigation, Formal analysis, Writing—original draft. Q.C.: Methodology, Writing—review and editing, Recourses. Y.L.: Methodology, Writing—review and editing. J.S.: Methodology, Writing—review and editing, Funding acquisition. All authors have read and agreed to the published version of the manuscript.

Funding: This work was financially supported by the Key Collaborative Research Program of the Alliance of International Science Organization (ANSO-CR-KP-2020-13); the National Natural Science Foundation of China (52072387); the Inner Mongolia Key R&D Plan (2022YFHH0049); the Shanghai Commission of Science and Technology Program (22ZR1471800); and the State Key Laboratory Director Fund of SICCAS (Y9ZC0102).

Institutional Review Board Statement: Not applicable.

Informed Consent Statement: Not applicable.

Data Availability Statement: The data presented in this study are available in this article.

Conflicts of Interest: The authors declare no conflict of interest.

References

1. Shukla, A.K.; Alam, J.; Mishra, U.; Kesari, K.K. Investigating the efficiency of a ceramic-based thin-film composite nanofiltration membrane for dyes removal. *Ceram. Int.* **2023**, *49*, 37670–37679. [CrossRef]
2. Li, C.; Li, S.; Zhang, J.; Yang, C.; Su, B.; Han, L.; Gao, X. Emerging sandwich-like reverse osmosis membrane with interfacial assembled covalent organic frameworks interlayer for highly-efficient desalination. *J. Membr. Sci.* **2020**, *604*, 118065. [CrossRef]
3. Ding, J.; Mao, Z.; Chen, H.; Zhang, X.; Fu, H. Fabrication of ZnO/PDA/GO composite membrane for high efficiency oil–water separation. *Appl. Phys. A* **2023**, *129*, 369. [CrossRef]
4. Sutrisna, P.D.; Kurnia, K.A.; Siagian, U.W.R.; Ismadji, S.; Wenten, I.G. Membrane fouling and fouling mitigation in oil–water separation: A review. *J. Environ. Chem. Eng.* **2022**, *10*, 107532. [CrossRef]
5. Zhang, H.; Guo, Z. Biomimetic materials in oil/water separation: Focusing on switchable wettabilities and applications. *Adv. Colloid Interface Sci.* **2023**, *320*, 103003. [CrossRef]
6. Wang, D.; Zhao, Z.; Qiao, C.; Yang, W.; Huang, Y.; McKay, P.; Yang, D.; Liu, Q.; Zeng, H. Techniques for treating slop oil in oil and gas industry: A short review. *Fuel* **2020**, *279*, 118482. [CrossRef]
7. Gupta, R.K.; Dunderdale, G.J.; England, M.W.; Hozumi, A. Oil/water separation techniques: A review of recent progresses and future directions. *J. Mater. Chem. A* **2017**, *5*, 16025–16058. [CrossRef]
8. Shi, Z.; Zhang, W.; Zhang, F.; Liu, X.; Wang, D.; Jin, J.; Jiang, L. Ultrafast separation of emulsified oil/water mixtures by ultrathin free-standing single-walled carbon nanotube network films. *Adv. Mater.* **2013**, *25*, 2422–2427. [CrossRef]
9. Zhang, R.; Liu, Y.; He, M.; Su, Y.; Zhao, X.; Elimelech, M.; Jiang, Z. Antifouling membranes for sustainable water purification: Strategies and mechanisms. *Chem. Soc. Rev.* **2016**, *45*, 5888–5924. [CrossRef]
10. Zhang, X.; Zhao, Y.; Mu, S.; Jiang, C.; Song, M.; Fang, Q.; Xue, M.; Qiu, S.; Chen, B. UiO-66-Coated Mesh Membrane with Underwater Superoleophobicity for High-Efficiency Oil-Water Separation. *ACS Appl. Mater. Interfaces* **2018**, *10*, 17301–17308. [CrossRef]
11. Zhang, J.; Peng, K.; Xu, Z.K.; Xiong, Y.; Liu, J.; Cai, C.; Huang, X. A comprehensive review on the behavior and evolution of oil droplets during oil/water separation by membranes. *Adv. Colloid Interface Sci.* **2023**, *319*, 102971. [CrossRef]
12. Abidli, A.; Huang, Y.; Park, C.B. In situ oils/organic solvents cleanup and recovery using advanced oil-water separation system. *Chemosphere* **2020**, *260*, 127586. [CrossRef] [PubMed]
13. Križan Milić, J.; Murić, A.; Petrinić, I.; Simonič, M. Recent Developments in Membrane Treatment of Spent Cutting-Oils: A Review. *Ind. Eng. Chem. Res.* **2013**, *52*, 7603–7616. [CrossRef]
14. Roy, B.; Dey, S.; Sahoo, G.C.; Roy, S.N.; Bandyopadhyay, S. Degumming, Dewaxing and Deacidification of Rice Bran Oil-Hexane Miscella Using Ceramic Membrane: Pilot Plant Study. *J. Am. Oil Chem. Soc.* **2014**, *91*, 1453–1460. [CrossRef]
15. Jia, H.; Feng, F.; Wang, J.; Ngo, H.-H.; Guo, W.; Zhang, H. On line monitoring local fouling behavior of membrane filtration process by in situ hydrodynamic and electrical measurements. *J. Membr. Sci.* **2019**, *589*, 117245. [CrossRef]
16. Maddela, N.R.; Torres, R.O.V. The presence of low fouling-causing bacteria can lead to decreased membrane fouling potentials of mixed cultures. *J. Environ. Chem. Eng.* **2021**, *9*, 105131. [CrossRef]
17. Marzouk, S.S.; Naddeo, V.; Banat, F.; Hasan, S.W. Preparation of TiO_2/SiO_2 ceramic membranes via dip coating for the treatment of produced water. *Chemosphere* **2021**, *273*, 129684. [CrossRef]
18. Li, Y.; Chen, H.; Wang, Q.; Li, G. Further modification of oil–water separation membrane based on chitosan and titanium dioxide. *J. Mater. Sci. Mater. Electron.* **2021**, *32*, 4823–4832. [CrossRef]
19. Chang, Q.; Zhou, J.-E.; Wang, Y.; Liang, J.; Zhang, X.; Cerneaux, S.; Wang, X.; Zhu, Z.; Dong, Y. Application of ceramic microfiltration membrane modified by nano-TiO_2 coating in separation of a stable oil-in-water emulsion. *J. Membr. Sci.* **2014**, *456*, 128–133. [CrossRef]
20. Meng, T.; Xie, R.; Ju, X.-J.; Cheng, C.-J.; Wang, S.; Li, P.-F.; Liang, B.; Chu, L.-Y. Nano-structure construction of porous membranes by depositing nanoparticles for enhanced surface wettability. *J. Membr. Sci.* **2013**, *427*, 63–72. [CrossRef]
21. Suresh, K.; Srinu, T.; Ghoshal, A.K.; Pugazhenthi, G. Preparation and characterization of TiO_2 and γ-Al_2O_3 composite membranes for the separation of oil-in-water emulsions. *RSC Adv.* **2016**, *6*, 4877–4888. [CrossRef]
22. Raji, Y.O.; Othman, M.H.D.; Sapiaa Md Nordin, N.A.H.; Adam, M.R.; Mohd Said, K.A.; Ismail, A.F.; Rahman, M.A.; Jaafar, J.; Farag, T.M.; Alftessi, S.A. Synthesis and characterization of superoleophobic fumed alumina nanocomposite coated via the sol-gel process onto ceramic-based hollow fibre membrane for oil-water separation. *Ceram. Int.* **2021**, *47*, 25883–25894. [CrossRef]
23. Usman, J.; Othman, M.H.D.; Ismail, A.F.; Rahman, M.A.; Jaafar, J.; Raji, Y.O.; Gbadamosi, A.O.; El Badawy, T.H.; Said, K.A.M. An overview of superhydrophobic ceramic membrane surface modification for oil-water separation. *J. Mater. Res. Technol.* **2021**, *12*, 643–667. [CrossRef]
24. Barati, N.; Husein, M.M.; Azaiez, J. Modifying ceramic membranes with in situ grown iron oxide nanoparticles and their use for oily water treatment. *J. Membr. Sci.* **2021**, *617*, 118641. [CrossRef]
25. Kaur, H.; Bulasara, V.K.; Gupta, R.K. Influence of pH and temperature of dip-coating solution on the properties of cellulose acetate-ceramic composite membrane for ultrafiltration. *Carbohydr. Polym.* **2018**, *195*, 613–621. [CrossRef]
26. Zhao, J.; Cao, L.; Wang, X.; Huo, H.; Lin, H.; Wang, Q.; Yang, X.; Vogel, F.; Li, W.; Lin, Z.; et al. MOF@Polydopamine-incorporated membrane with high permeability and mechanical property for efficient fouling-resistant and oil/water separation. *Environ. Res.* **2023**, *236 Pt 2*, 116685. [CrossRef]

27. Liu, Z.; Ma, W.; Zhang, M.; Zhang, Q.; Xiong, R.; Huang, C. Fabrication of superhydrophobic electrospun polyimide nanofibers modified with polydopamine and polytetrafluoroethylene nanoparticles for oil–water separation. *J. Appl. Polym. Sci.* **2019**, *136*, 47638. [CrossRef]
28. Gao, N.; Wang, L.; Zhang, Y.; Liang, F.; Fan, Y. Modified ceramic membrane with pH/ethanol induced switchable superwettability for antifouling separation of oil-in-acidic water emulsions. *Sep. Purif. Technol.* **2022**, *293*, 121022. [CrossRef]
29. Li, Y.; He, Y.; Zhuang, J.; Shi, H. An intelligent natural fibrous membrane anchored with ZnO for switchable oil/water separation and water purification. *Colloids Surf. A Physicochem. Eng. Asp.* **2022**, *634*, 128041. [CrossRef]
30. Chew, N.G.P.; Zhao, S.; Malde, C.; Wang, R. Superoleophobic surface modification for robust membrane distillation performance. *J. Membr. Sci.* **2017**, *541*, 162–173. [CrossRef]
31. Tian, Y.; Cao, Y.; Wang, Y.; Yang, W.; Feng, J. Realizing ultrahigh modulus and high strength of macroscopic graphene oxide papers through crosslinking of mussel-inspired polymers. *Adv. Mater.* **2013**, *25*, 2980–2983. [CrossRef]
32. Yang, H.-C.; Liao, K.-J.; Huang, H.; Wu, Q.-Y.; Wan, L.-S.; Xu, Z.-K. Mussel-inspired modification of a polymer membrane for ultra-high water permeability and oil-in-water emulsion separation. *J. Mater. Chem. A* **2014**, *2*, 10225–10230. [CrossRef]
33. Luan, W.; Nie, C.; Chen, X.; Tang, Z.; Qiu, M.; Fan, Y. Effective construction of anti-fouling zwitterion-functionalized ceramic membranes for separation of oil-in-water emulsion based on PDA/PEI co-deposition. *J. Environ. Chem. Eng.* **2022**, *10*, 108396. [CrossRef]
34. Zhao, C.; Yu, X.; Da, X.; Qiu, M.; Chen, X.; Fan, Y. Fabrication of a charged PDA/PEI/Al_2O_3 composite nanofiltration membrane for desalination at high temperatures. *Sep. Purif. Technol.* **2021**, *263*, 118388. [CrossRef]
35. Song, H.-M.; Chen, C.; Shui, X.-X.; Yang, H.; Zhu, L.-J.; Zeng, Z.-X.; Xue, Q.-J. Asymmetric Janus membranes based on in situ mussel-inspired chemistry for efficient oil/water separation. *J. Membr. Sci.* **2019**, *573*, 126–134. [CrossRef]
36. Naik, R.R.; Whitlock, P.W.; Rodriguez, F.; Brott, L.L.; Glawe, D.D.; Clarson, S.J.; Stone, M.O. Controlled formation of biosilica structures in vitro. *Chem. Commun.* **2003**, 238–239. [CrossRef] [PubMed]
37. Yang, H.C.; Pi, J.K.; Liao, K.J.; Huang, H.; Wu, Q.Y.; Huang, X.J.; Xu, Z.K. Silica-decorated polypropylene microfiltration membranes with a mussel-inspired intermediate layer for oil-in-water emulsion separation. *ACS Appl. Mater. Interfaces* **2014**, *6*, 12566–12572. [CrossRef]
38. Gao, N.; Fan, W.; Xu, Z.-K. Ceramic membrane with protein-resistant surface via dopamine/diglycolamine co-deposition. *Sep. Purif. Technol.* **2020**, *234*, 116135. [CrossRef]
39. Liu, G.; Yang, Y.; Liu, H.; Wang, Q.; Wang, Y.; Zhou, J.-E.; Chang, Q. Preparation of disc ceramic membrane by a printing and dip-coating method for oil-water separation. *Sep. Purif. Technol.* **2023**, *315*, 123552. [CrossRef]
40. Qu, Y.; Qin, L.; Guo, M.; Liu, X.; Yang, Y. Multilayered molecularly imprinted composite membrane based on porous carbon nanospheres/pDA cooperative structure for selective adsorption and separation of phenol. *Sep. Purif. Technol.* **2022**, *280*, 119915. [CrossRef]
41. Liang, Q.; Jiang, B.; Yang, N.; Zhang, L.; Sun, Y.; Zhang, L. Superhydrophilic Modification of Polyvinylidene Fluoride Membrane via a Highly Compatible Covalent Organic Framework-COOH/Dopamine-Integrated Hierarchical Assembly Strategy for Oil-Water Separation. *ACS Appl. Mater. Interfaces* **2022**, *14*, 45880–45892. [CrossRef] [PubMed]
42. Nagasawa, H.; Omura, T.; Asai, T.; Kanezashi, M.; Tsuru, T. Filtration of surfactant-stabilized oil-in-water emulsions with porous ceramic membranes: Effects of membrane pore size and surface charge on fouling behavior. *J. Membr. Sci.* **2020**, *610*, 118210. [CrossRef]